SCIENCE CHINA
Life Sciences

• RESEARCH PAPERS •

June 2010 Vol.53 No.6: 669–676
doi: 10.1007/s11427-010-4004-6

Properties of mouse retinal ganglion cell dendritic growth during postnatal development

YANG XiuLan, SHI XiangMing & HE ShiGang*

State Key Laboratory of Brain and Cognitive Sciences, Institute of Biophysics, Chinese Academy of Sciences, Beijing 100101, China

Received February 21, 2010; accepted March 26, 2010

The property of dendritic growth dynamics during development is a subject of intense interest. Here, we investigated the dendritic motility of retinal ganglion cells (RGCs) during different developmental stages, using *ex vivo* mouse retina explant culture, Semliki Forest Virus transfection and time-lapse observations. The results illustrated that during development, the dendritic motility underwent a change from rapid growth to a relatively stable state, i.e., at P0 (day of birth), RGC dendrites were in a highly active state, whereas at postnatal 13 (P13) they were more stable, and at P3 and P8, the RGCs were in an intermediate state. At any given developmental stage, RGCs of different types displayed the same dendritic growth rate and extent. Since the mouse is the most popular mammalian model for genetic manipulation, this study provided a methodological foundation for further exploring the regulatory mechanisms of dendritic development.

retinal ganglion cells, dendritic development, time-lapse observation

Citation: Yang X L, Shi X M, He S G. Properties of mouse retinal ganglion cell dendritic growth during postnatal development. Sci China Life Sci, 2010, 53: 669−676, doi: 10.1007/s11427-010-4112-3

The retina, as part of and like many other central nervous system structures, contains a huge diversity of neuronal types. It is a suitable preparation for many studies because it can be isolated as an intact sheet of tissue without disrupting its structure or function. In this study, we focused on the output neurons of the retina, the retinal ganglion cells (RGCs). Based on their branching level, dendritic arbor width and electrophysiological properties, RGCs in the different species of adult mammals that have been investigated to date could always be classified into 10 to 15 different groups, e.g., cats [1], rabbits [2], rats [3], mice [4,5] and chickens [6]. Each type of RGCs has its own specific upstream synaptic partners, that is, bipolar cells or amacrine cells, to extract a certain aspect of information from the visual scene [7]. During early development, it is another scenario, and many studies have detected RGC developmental changes in a variety of species, including transient features, dendritic remodeling and stratification [8–29]. However, only a few studies had been undertaken to examine the dendritic motility of RGCs during the different developmental stages [23,24], and these were performed in chicken embryo RGCs.

Here, we studied the mouse retina because of its many advantages for genetic manipulation. In the first 14 d after mouse birth, profound remodeling takes place to render the adult morphology of RGCs. Mouse RGCs at the time of birth (P0) cannot be classified based on the criteria developed for adult RGCs. They are not well differentiated and their dendrites diffusely stratify in the inner plexiform layer (IPL). The cholinergic stratification can first be detected at P3 [30], and the morphology of RGCs at this time is almost the same as that of P0 RGCs, with the exception that the RGC stratification is tighter, although still diffuse in the IPL. P0 and P3 RGCs are divided into simple RGCs and complex RGCs, depending on the complexity of the dendritic field. However, at P8, before bipolar cells make synaptic

*Corresponding author (email: shiganghe@moon.ibp.ac.cn)

contacts with RGCs [31], 80.7% of RGCs develop an adult-like morphology and stratification, and at P13, before eye-opening to receive well-focused light stimuli, the majority of RGCs can be classified into one of the 14 adult subtypes. In this study, we were particularly interested in the dendritic remodeling during the above-mentioned developmental stages, and aimed to investigate whether there is any difference in dendritic motility between the distinct types of RGCs at the same developmental stage, and whether dendritic motility varied among different developmental stages.

1 Materials and methods

1.1 Retina isolation and Semliki Forest Virus (SFV) transfection

C57BL/6N mice were used in this study. The use and handling of animals were strictly in accordance with the institutional guidelines of the Institute of Biophysics, Chinese Academy of Sciences and with the Association for Research in Vision and Ophthalmology statement for the Use of Animals in Ophthalmic and Vision Research. The procedure for retina isolation was as previously described [11]. Briefly, mice at postnatal day 0, 3, 8, and 13 were deeply anesthetized by hypothermia, the eyes quickly enucleated, and the animals subsequently sacrificed. A slit was cut in the sclera close to the cornea, and the eyes then submerged in oxygenated Ames' medium, which contains 43 chemicals including inorganic salts, amino acids, and vitamins, and which was formulated to support retinal tissue in relatively short-term culture. The retina incubated in Ames' medium for more than 2 d maintained its metabolism and electrical responses to photic stimuli [32].

The front part (the cornea, lens, and vitreous) of the eye was discarded and the retina was carefully isolated from the pigment epithelium under a Nikon SMZ660 dissecting microscope. A few radial slits were cut in the retina to flatten it. The retina was attached, ganglion cell side up, on a black Millipore filter (AABP02500), incubated in the oxygenated Ames' medium, and was then ready for transfection.

The retina with the filter was placed on an autoclaved normal filter, and as much excess Ames' medium as possible was drained. The retina with the filter was placed in a culture dish and 1 μL 1×10^9 SFV (Shanghai GeneChem Co., Ltd) was added. The dish was then moved to a cell incubator. Five min later, 5 μL Ames' medium was added to the retina, and 20 min after this another 20 μL medium was added to prevent the retina from drying. Then, the retina with the filter was transferred to the *in vitro* perfusion system with 35°C Ames' medium equilibrated with 95% O_2 and 5% CO_2 at a rate of 6 mL min^{-1}. Individual green florescent protein (GFP)-positive RGCs with a fine structure of dendrites and axons were observed after 10–12 hours' transfection.

1.2 Electrophysiological recording

To detect whether the RGCs were physiologically intact after *in vitro* culture and SFV transfection, spontaneous activities of the RGCs were recorded. The procedure was as previously described [9]. The retina was carefully detached from the black Millipore filter and reattached, ganglion cell side up, to another piece of black Millipore filter paper (AABP02500) with a 2 mm diameter hole in the centre for infrared illumination. The whole-mount retinal preparation was then transferred into a recording chamber (0.5 mL in volume) on the fixed stage of an upright microscope (Leica DMLFSA) equipped with a 40× water-immersion objective, a fluorescent illumination system and a CCD camera. The preparation was continuously superfused at a rate of 6 mL min^{-1} in 35°C $NaHCO_3$-buffered Ames' medium equilibrated with 95% O_2 and 5% CO_2.

Micropipettes were manufactured from thick-walled borosilicate filament glass tubing using a Flaming-Brown P97 puller (Sutter Instruments Inc., Novato, CA, USA). Under infrared illumination and visual control through a cooled CCD camera (Sensicam, Cooke, Auburn Hills, Mi, USA), the Müller cell end-feet and inner limiting membrane in the selected region with GFP-positive cells were dissected with a pipette to expose the somata of several RGCs. The pipette used to dissect the cells was replaced with a pipette filled with Ames' medium (2–4 MΩ). Gentle suction was applied to establish a loose-patch configuration and spike activities were recorded. The bursts of the RGCs that were GFP-positive and -negative were respectively recorded. Data acquired from the Axopatch 200B amplifier were low-pass filtered at 2 kHz, digitized simultaneously with an A/D converter (Digidata 1322A, Axon Instruments), and stored on a personal computer. Data analysis was performed offline using Clampfit (Axon Instruments) and Mini Analysis (Synaptosoft Inc., Leonia, NJ, USA), and figures were plotted with OriginPro 7.0 (MicroCal Software Inc., Northampton, MA, USA).

1.3 Time-lapse imaging

Transfected retinae with labeled cells were transferred to a stage-mounted, temperature-controlled (35°C) chamber with oxygenated artificial cerebrospinal fluid (ACSF) continuously superfused (6 mL min^{-1}). ACSF was composed of (in mmol L^{-1}): 124 NaCl, 3.4 KCl, 1.7 $MgSO_4$, 1.4 NaH_2PO_4, 1.9 $CaCl_2{\cdot}2H_2O$, 10 Glucose, 25 $NaHCO_3$, pH 7.4. The chamber was placed on a Nikon ECLIPSE E800 microscope equipped with a Photometrics Cascade 512B camera (Roper Scientific, Inc.) and images were collected with a Nikon Plan APO 40× (N.A. 0.85) water-immersion objective. Ganglion cells with well resolved arbors were chosen for time-lapse imaging. Time-lapse images of den-

dritic arbors of interest were reconstructed as a sequence of *z*-projections from stacks of optical sections spanning the entire *z*-dimension of the cell captured every minute for a total period of 15 min.

1.4 Data analysis

Metamorph (Universal Imaging Corporation) was used for measurement of the lengths of the final branches. We adopted the system of evaluation used by Wong [23]. To follow the length of a process over time, we measured the length of the final branch, i.e., from the process tip to its base, in each image separately. The lifetime of an individual process was estimated to be the total period across a recording for which the process was evident. The rate and extent of dendritic movements were computed by following the changes in the length of an individual process across the recording period or, for non-persistent processes, the duration over which the process was present. The mean rate of an individual process was calculated as:

$$\sum_{t=0}^{n} | L_{t+1} - L_t | / D(\text{time interval} = 1 \text{ min for } 15 \text{ min}), \quad (1)$$

where L_t and L_{t+1} are the length of each process at time point t and t+1 respectively, n is the total number of time points, and D is the total time for which each process was monitored. The average rate for multiple processes in one or several RGCs is simply the sum of the individual rate divided by the number of processes. The mean motility extent of processes in one or several RGCs was calculated as:

$$\sum_{i=1}^{n} | L_{i,\max} - L_{i,\min} | / n \text{ (time period=15 min)}, \quad (2)$$

where $L_{i,\max}$ and $L_{i,\min}$ are the maximum and minimum length of each process during the recorded time period, n is the total number of the recorded processes and i indicates the number given to individual processes, e.g., 1, 2, 3... to facilitate the analysis.

1.5 Statistics

All data were expressed as mean±SEM. One-way analysis of variance with Student-Newman-Keuls post-hoc test was performed on motility rate and extent of different types of RGCs or of RGCs of different developmental stages. $P \leqslant 0.05$ was considered to indicate a significant difference.

2 Results

2.1 SFV-transfected RGCs display rapid dendritic remodeling

SFV is a plus-strand RNA virus belonging to the alphavirus genus. Vectors for SFV have been developed to express high levels of foreign gene *in vitro* and *in vivo* [33]. In the present study, we selected SFV due to its high-affinity for neurons, as well as its capabilities for fast, high and transient gene expression. GFP expression in RGCs in this study was first detectable after 5–6 h of transfection, and complete labeling of ganglion cells arbors was observed 10–12 h after transfection. A P0 RGC with well-resolved dendritic arbors is illustrated in Figure 1A. The dendritic remodeling in these GFP-positive cells was robust; as shown in Figure 1B, at 2 min intervals for a total of only 8 min, dendritic changes involved extensions and retractions of processes, as well as the addition of new processes and elimination of existing processes. These different forms of reorganization occurred simultaneously in all parts of the dendritic tree and were prominent and rapid for the duration of the recording. This reorganization was primarily restricted to the final (or tertiary) branches, while the primary and secondary branches changed little if at all.

2.2 Dendritic remodeling occurred in spontaneously-active cells

Previous studies [34] showed that, during the developmental stages we investigated, there were spontaneous rhythmic-bursting activities that propagate horizontally across the retina in the form of waves every 1–2 min. The RGCs produce action potentials when they undergo spontaneous activities, and the propagation of spontaneous activities depends on the release of neurotransmitters inside the functional synapses, and gap junction coupling between neurons [35]. To detect whether the above-observed rapid dendritic remodeling occurred in physiologically intact retina, a patch-clamp study was undertaken to examine the activity of GFP-positive and GFP-negative RGCs in P8 retina after 17 hours' transfection. Figure 2 shows that the GFP-labeled ganglion cell fired in a similar manner to its non-transfected neighbor, and bursts occurred in all cells about once every 1–2 min. Thus, the restructuring events we observed are likely to be representative of those occurring in intact circuits.

2.3 No difference in dendritic motility was detected between different types of RGCs at any given developmental stage

Having observed continuous movements of the dendritic processes and confirmed that these dendritic motilities represent the physiological dendritic growth in intact retina, we used two parameters to quantify their dynamics. First, we calculated motility rate, which is the sum of the process length changes across the recording period divided by the time that the process was present (defined mathematically in Materials and methods). This parameter indicated the velocity of a particular process changed. Second, we measured the extent of movement, which is defined as the difference between the maximum and minimum lengths exhibited by a

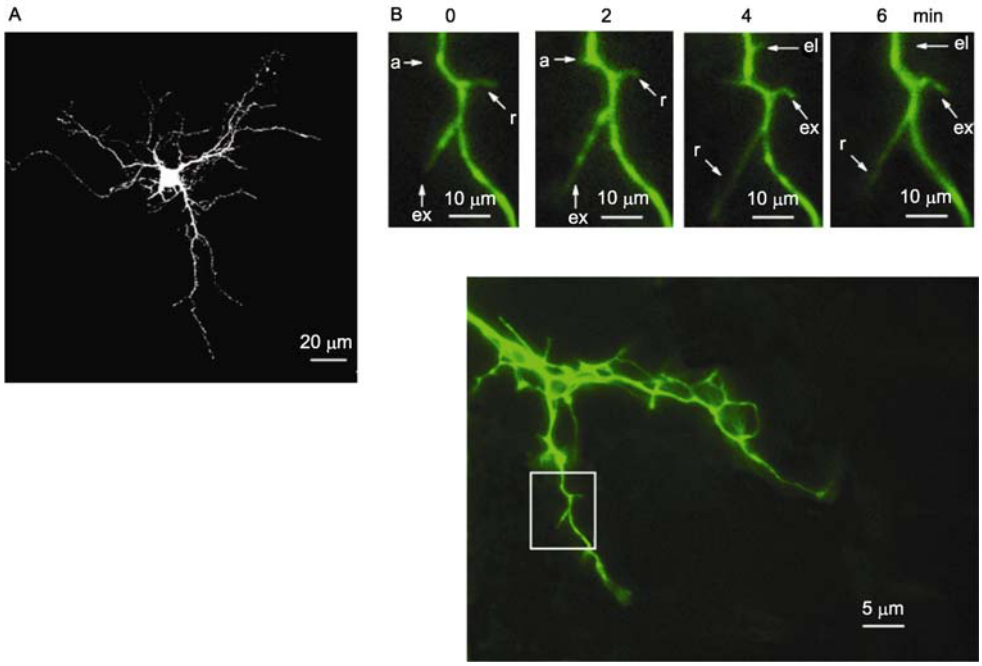

Figure 1 SFV-transfected P0 RGCs and dendritic remodeling. A, morphology of one complex P0 RGC after 12 h transfection. Scale bar is 20 μm. B, rapid dendritic remodeling images taken 2 min apart. Structural changes include extensions (ex), retractions (r), addition of new processes (a), and elimination of previously-existing processes (el).

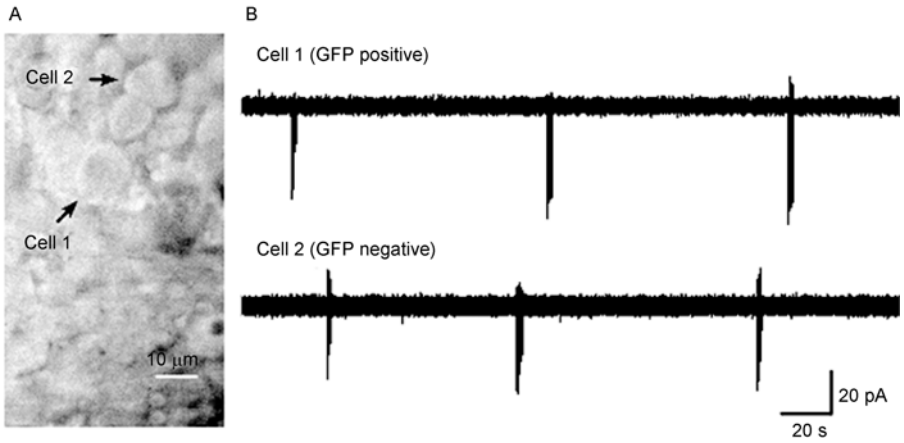

Figure 2 Dendritic remodeling occurs in intact, endogenously active retinal circuits. A, somas of some P8 RGCs after 17 h transfection; cell 1 was SFV-transfected while cell 2 was not. B, similarly regular electric activity for each of these two cells.

process across the recording period of 15 min. This parameter reflected the "reach" achieved by a process over a few minutes.

2.3.1 Dendritic growth of P0 retinal ganglion cells

Eleven RGCs from six P0 retinae were analyzed. As mentioned above, it was impossible to classify P0 RGCs using criteria developed for the adult. Therefore, simply based on the number of dendritic branching points throughout their dendritic field (with branches defined as having a minimum length of 2.5 μm), the 11 RGCs were divided into two groups: simple RGCs (with less than 25 branching points) and complex RGCs (with more than 25 branching points). Among the 11 cells analyzed, five were simple RGCs with branching points numbering 15.8±1.8, ranging from 12 to 20; and the other six were complex RGCs with branching points numbering 40.3±3.3, ranging from 36 to 56. The dendritic remodeling rate and extent of these five simple and six complex RGCs were examined separately and statistically analyzed, and no difference was found for the two types of RGCs (Figure 3A).

2.3.2 Dendritic remodeling of P3 retinal ganglion cells

Nine RGCs from six P3 retinae were collected in this group.

Similar to P0 RGCs, we classified the nine RGCs into simple and complex groups. Four were simple RGCs with 19.8±0.9 branching points, ranging from 18 to 22; while the other five were complex RGCs with 51.4±4.1 branching points, ranging from 39 to 62. The dendritic motility rate and extent of these four simple and five complex RGCs were examined separately and statistically analyzed, and no difference was detected between these two RGC types (Figure 3B).

2.3.3 Dendritic dynamics of P8 retinal ganglion cells

At P8, even before RGCs receive the synaptic input from bipolar cells, most of the RGCs can be classified using criteria developed for the adult. Previous study in the mouse retina [29] showed that different RGCs exhibited different modes of growth rate compared with the growth rate of the eyeball from P8 to adult. We wondered whether the dendritic dynamics were different for distinct types of RGCs. Twelve RGCs from eight retinae were analyzed and all of these could be clearly classified; four were A-type, five were B-type and the other three was C-type RGCs. The rate and extent of dendritic motility were analyzed, and unexpectedly, no difference was detected among the different types of RGCs (Figure 3C).

2.3.4 Dendritic motility of P13 retinal ganglion cells

At P13, the retina is ready to receive well-focused light stimuli, and a predominant number of RGCs possess their adult morphology. Twelve RGCs from seven retinae were analyzed, and among them, five were A-type, four were B-type and three were C-type RGCs.

The rate and extent of dendritic motility were analyzed, and similarly to the results described above, no difference was found among the different types of RGCs (Figure 3D).

2.4 Dendritic growth is developmentally regulated

Gathering the data together, the difference (Figure 4) among the different developmental stages became apparent: P0 RGCs were in a highly active state, whereas at P13 the RGCs had became relatively stable, and P3 and P8 RGCs were in an intermediate state with no difference between P3 and P8 RGC dendritic growth dynamics. In summary, dendritic remodeling of RGCs underwent a process of gradually decreasing during development, with the rate changing from (0.83±0.05) μm min^{-1} at P0 to (0.37±0.03) μm min^{-1} at P13, and the extent changing from (3.38±0.12) μm at P0 to (1.50±0.11) μm at P13, during the 15 min of recording. Therefore, we conclude that the rapid dendritic movements observed are a feature of immature cells and that they are developmentally regulated.

3 Discussion

To investigate the dendritic growth properties of mouse RGCs during the different developmental periods and to further explore the possible regulators that may modulate the developmental process, dendritic growth rate and extent were comprehensively characterized in this study. The den-

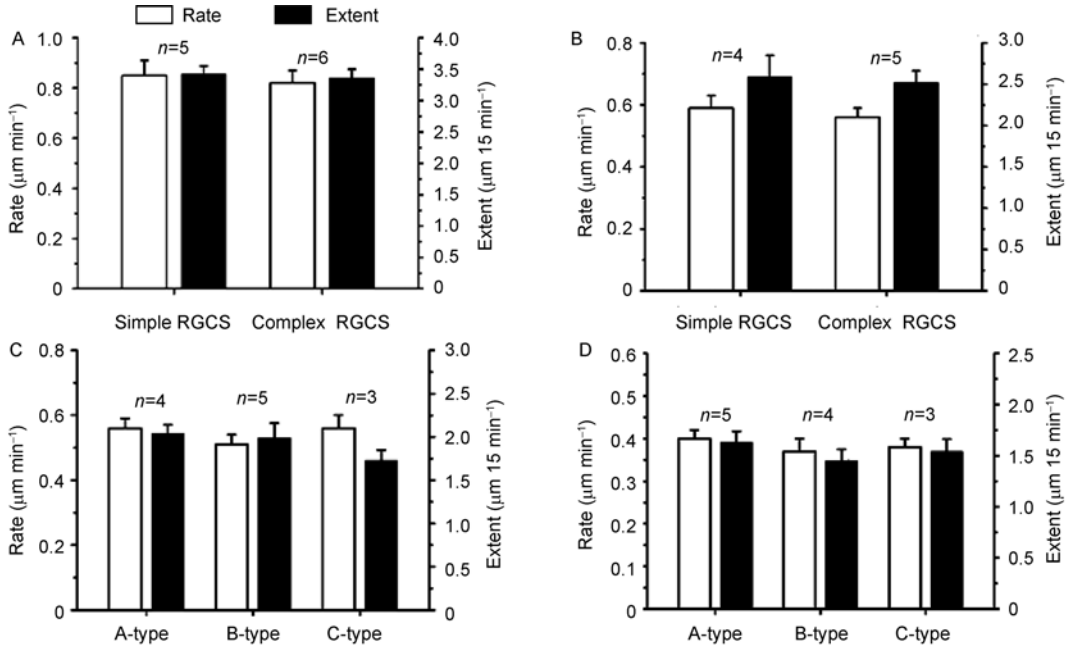

Figure 3 Properties of dendritic growth of different types of RGCs during distinct developmental stages. A, B, C and D represent the dendritic remodeling of P0, P3, P8 and P13 RGCs, respectively. They show that at any given developmental stage, there is no difference in dendritic growth rate and extent among the different types of RGCs, within our 15 min of recording. N indicates the number of cells analyzed in each case.

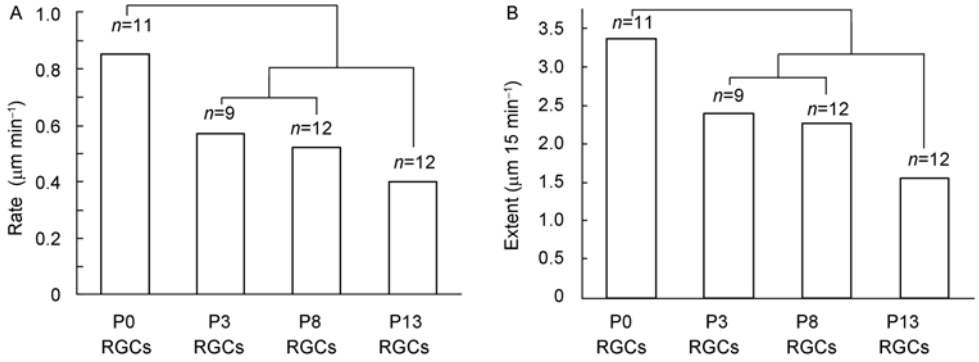

Figure 4 Dendritic remodeling is developmentally regulated. A and B show the changes of dendritic motility rate and extent, respectively, during development. Clearly, dendritic remodeling undergoes a process of rapid growth before decreasing to a relatively stable state. *N* represents the number of cells analyzed in each case.

dritic remodeling rate and extent of RGCs underwent a process of gradually decreasing during development from P0 to P13, and we did not detect a difference in dendritic dynamics among the different RGC types at any developmental stage.

3.1 Dendritic motility during different developmental stages

Our observations illustrate that during the developmental period from P0 to P13, RGC dendrites undergo rapid remodeling, though motility decreases as development proceeds. The dendritic motility is most active at P0, at which time the whole retina is still primitive. Though amacrine cells and ganglion cells have differentiated [36,37], their morphologies are far from mature [11], i.e., they are small in size, their processes are distributed diffusely in the IPL, and the retina is not yet ready to establish any synapses. Further, vesicular acetylcholine transporter (VAchT) staining, which reveals the cholinergic plexuses of amacrine cells in the IPL, is sparsely and diffusely distributed in the IPL [30]. There is no direct evidence regarding the density of processes in the IPL of P0 mouse retina. However, an electron microscopy study [38] of embryo chicken retinae at E10 shows that the processes in IPL appear to be independent of each other, there are some free spaces between processes, and no synapses have yet formed. If the situation is comparable between mouse retina and chicken retina, it may be possible that the free spaces in P0 mouse retina IPL lead to the high activity of the dendritic processes. Clearly though, direct evidence is needed to confirm this possibility.

At P3, the earliest indication of cholinergic ON- and OFF-stratification of amacrine cells in IPL occurs, as showed by VAchT staining [30]. Meanwhile, the synapses between amacrine cells and ganglion cells are beginning to form [39–41], which indicates there are direct contacts and synapse formation on the dendritic processes of RGCs at this time. This may lead to the limitation in dendritic motility and may explain why there is such a large difference between P0 and P3 RGC dendritic dynamics. At P8, bipolar cells are well differentiated [42] and ready to make synapses with RGCs, while there is no difference in dendritic motility at P8 when compared with P3, indicating that the dendritic processes have the same growth properties during synapse formation irrespective of whether they are cholinergic or glutamatergic synapses. These results are consistent with those of Wong's study on chicken embryo retinae [24]. The retinae reach an almost mature stage at P13, and most of the synapses are sufficiently well formed to receive well-focused light stimulation on the following day. At this time point, the dendritic growth rate and extent decrease dramatically, and the processes are in a relatively stable state. Therefore, our study clearly shows that after birth, as the mouse RGCs reach a mature state, dendritic dynamics undergoes a change from an active to a relatively stable condition.

In this study, we did not observe dendritic dynamic differences between distinct RGCs at any given developmental stage, which is consistent with the study of RGCs in chicken embryo [23,24] examining dendritic motility during the different developmental stages. As mentioned previously, RGCs in the chicken can also be divided into distinct groups [6,43,44], and one study has indicated that chicken RGCs may experience a similar growth process to mouse RGCs [10]. It was also found that there was no dendritic motility difference between the different types of RGCs. It appears that the activity in the IPL may occur synchronously to different types of RGCs, while another possibility could be that due to the limited 15 min period of observation, we failed to observe existing differences between distinct RGCs at certain developmental stages. Furthermore, in this study, dendritic remodeling mostly occurred in the tertiary branches and almost no changes in primary or secondary branches were observed. We assume that prolonging the culture and observation period should enable detection of differences between distinct RGCs, which would be an in-

teresting project to undertake in the future.

3.2 Possible modulators of developmentally-regulated dendritic remodeling

Over the past several years, dendritic development has received a huge amount of attention, and accordingly numerous factors have been identified that influence dendritic growth and arborization. For example, intrinsic transcription factors as well as extracellular signals can affect dendritic growth [45]. As for the visual system, visual experience [21,25,46–50] can also influence dendritic growth. All of these factors may cause changes in the cytoskeleton, macromolecule synthesis and membrane turnover, which eventually influences dendritic growth. These factors may act independently, but it is more reasonable to assume that they work together orchestrally. It is possible that the dendritic dynamics observed in this study was regulated by some or all of these factors. For example, it has been established that neurotransmitters during different developmental stages modulate dendritic remodeling [24]. At E9–11, during which time synapses are formed between amacrine cells and ganglion cells in the chicken embryo, application of DHβE (a nicotinic cholinergic antagonist) dramatically decreased the dendritic growth while treatment of the retinae with the glutamatergic blockers NBQX and APV had no effect. However, at E12–13, during the period of synapse formation between bipolar and ganglion cells, application of NBQX and APV decreased the dendritic growth rate and extent, indicating that glutamate from bipolar cells regulates RGC dendritic growth; by contrast, application of DHβE at this time had no effect on dendritic dynamics. Therefore, even though the dendritic motility properties were not different between these two stages, they are under the control of different modulators. While evidence has shown that the numerous above-mentioned factors influence dendritic arborization, it would be an interesting avenue to pursue how they affect dendritic motility, and if they function differently during different developmental stages. This study provides a perfect model by which dendritic remodeling can be recorded in the intact neuronal circuitry, and represents the situation *in vivo* much better than *ex vivo* cultured neurons, for further investigation of the factors that modulate dendritic motility.

We thank Liu ZhiPing and Liang HaiTian of the Institute of Biophysics for technical support. This work was supported by the National Basic Research Program of China (*Grant Nos. 2007CB512208 and 2006CB911003*).

1 Pu M, Berson D M, Pan T. Structure and function of retinal ganglion cells innervating the cat's geniculate wing: An *in vitro* study. J Neurosci, 1994, 14: 4338–4358
2 Rockhill R L, Daly F J, MacNeil M A, *et al*. The diversity of ganglion cells in a mammalian retina. J Neurosci, 2002, 22: 3831–3843
3 Sun W, Li N, He S. Large-scale morophological survey of rat retinal ganglion cells. Vis Neurosci, 2002, 19: 483–493
4 Sun W, Li N, He S. Large-scale morphological survey of mouse retinal ganglion cells. J Comp Neurol, 2002, 451: 115–126
5 Kong J H, Fish D R, Rockhill R L, *et al*. Diversity of ganglion cells in the mouse retina: unsupervised morphological classification and its limits. J Comp Neurol, 2005, 489: 293–310
6 Chen Y, Naito J. Morphological properties of chick retinal ganglion cells in relation to their central projections. J Comp Neurol, 2009, 514: 117–130
7 Masland R H. The fundamental plan of the retina. Nat Neurosci, 2001, 4: 877–886
8 Bodnarenko S R, Jeyarasasingam G, Chalupa L M. Development and regulation of dendritic stratification in retinal ganglion cells by glutamate-mediated afferent activity. J Neurosci, 1995, 15: 7037–7045
9 Chen M, Weng S, Deng Q, *et al*. Physiological properties of direction-selective ganglion cells in early postnatal and adult mouse retina. J Physiol, 2009, 587: 819–828
10 Chen Y, Hu M, Shibata H, *et al*. Changes in somal growth and dendritic patterns of the retinal ganglion cells in the chicks and chick embryos. J Vet Med Sci, 2003, 65: 1135–1137
11 Diao L, Sun W, Deng Q, *et al*. Development of the mouse retina: Emerging morphological diversity of the ganglion cells. J Neurobiol, 2004, 61: 236–249
12 Leventhal A G, Schall J D, Ault S J. Extrinsic determinants of retinal ganglion cell structure in the cat. J Neurosci, 1988, 8: 2028–2038
13 Liets L C, Olshausen B A, Wang G Y, *et al*. Spontaneous activity of morphologically identified ganglion cells in the developing ferret retina. J Neurosci, 2003, 23: 7343–7350
14 Lin B, Wang S W, Masland R H. Retinal ganglion cell type, size, and spacing can be specified independent of homotypic dendritic contacts. Neuron, 2004, 43: 475–485
15 Maslim J, Webster M, Stone J. Stages in the structural differentiation of retinal ganglion cells. J Comp Neurol, 1986, 254: 382–402
16 Mumm J S, Godinho L, Morgan J L, *et al*. Laminar circuit formation in the vertebrate retina. Prog Brain Res, 2005, 147: 155–169
17 Mumm J S, Williams P R, Godinho L, *et al*. *In vivo* imaging reveals dendritic targeting of laminated afferents by zebrafish retinal ganglion cells. Neuron, 2006, 52: 609–621
18 Perry V H, Linden R. Evidence for dendritic competition in the developing retina. Nature, 1982, 297: 683–685
19 Ramoa A S, Campbell G, Shatz C J. Dendritic growth and remodeling of cat retinal ganglion cells during fetal and postnatal development. J Neurosci, 1988, 8: 4239–4261
20 Ramoa A S, Yamasaki E N. Transient retinal ganglion cells in the developing rat are characterized by specific morphological properties. J Comp Neurol, 1996, 368: 582–596
21 Tian N. Synaptic activity, visual experience and the maturation of retinal synaptic circuitry. J Physiol, 2008, 586: 4347–4355
22 Weber A J, Kalil R E, Stanford L R. Dendritic field development of retinal ganglion cells in the cat following neonatal damage to visual cortex: Evidence for cell class specific interactions. J Comp Neurol, 1998, 390: 470–480
23 Wong W T, Faulkner-Jones B E, Sanes J R, *et al*. Rapid dendritic remodeling in the developing retina: dependence on neurotransmission and reciprocal regulation by Rac and Rho. J Neurosci, 2000, 20: 5024–5036
24 Wong W T, Wong R O. Changing specificity of neurotransmitter regulation of rapid dendritic remodeling during synaptogenesis. Nat Neurosci, 2001, 4: 351–352
25 Xu H P, Tian N. Retinal ganglion cell dendrites undergo a visual activity-dependent redistribution after eye opening. J Comp Neurol, 2007, 503: 244–259
26 Yamagata M, Sanes J R. Dscam and Sidekick proteins direct lamina-specific synaptic connections in vertebrate retina. Nature, 2008, 451: 465–469
27 Yamagata M, Weiner J A, Sanes J R. Sidekicks: Synaptic adhesion molecules that promote lamina-specific connectivity in the retina.

Cell, 2002, 110: 649–660
28 Yamasaki E N, Ramoa A S. Dendritic remodelling of retinal ganglion cells during development of the rat. J Comp Neurol, 1993, 329: 277–289
29 Ren L, Liang H, Diao L, *et al*. Changing dendritic field size of mouse retinal ganglion cells in early postnatal development. Dev Neurobiol, 2010, 70: 397–407
30 Stacy R C, Wong R O. Developmental relationship between cholinergic amacrine cell processes and ganglion cell dendrites of the mouse retina. J Comp Neurol, 2003, 456: 154–166
31 Sherry D M, Wang M M, Bates J, *et al*. Expression of vesicular glutamate transporter 1 in the mouse retina reveals temporal ordering in development of rod vs. cone and ON vs. OFF circuits. J Comp Neurol, 2003, 465: 480–498
32 Flores-Herr N, Protti D A, Wassle H. Synaptic currents generating the inhibitory surround of ganglion cells in the mammalian retina. J Neurosci, 2001, 21: 4852–4863
33 Ehrengruber M U, Lundstrom K, Schweitzer C, *et al*. Recombinant Semliki Forest virus and Sindbis virus efficiently infect neurons in hippocampal slice cultures. Proc Natl Acad Sci USA, 1999, 96: 7041–7046
34 Bansal A, Singer J H, Hwang B J, *et al*. Mice lacking specific nicotinic acetylcholine receptor subunits exhibit dramatically altered spontaneous activity patterns and reveal a limited role for retinal waves in forming ON and OFF circuits in the inner retina. J Neurosci, 2000, 20: 7672–7681
35 Blankenship A G, Feller M B. Mechanisms underlying spontaneous patterned activity in developing neural circuits. Nat Rev Neurosci, 2010, 11: 18–29
36 Cepko C L, Austin C P, Yang X, *et al*. Cell fate determination in the vertebrate retina. Proc Natl Acad Sci USA, 1996, 93: 589–595
37 Young R W. Cell differentiation in the retina of the mouse. Anat Rec, 1985, 212: 199–205
38 Hering H, Kroger S. Formation of synaptic specializations in the inner plexiform layer of the developing chick retina. J Comp Neurol, 1996, 375: 393–405
39 Fisher L J. Development of synaptic arrays in the inner plexiform layer of neonatal mouse retina. J Comp Neurol, 1979, 187: 359–372
40 McArdle C B, Dowling J E, Masland R H. Development of outer segments and synapses in the rabbit retina. J Comp Neurol, 1977, 175: 253–274
41 Olney J W. An electron microscopic study of synapse formation, receptor outer segment development, and other aspects of developing mouse retina. Invest Ophthalmol, 1968, 7: 250–268
42 Morgan J L, Dhingra A, Vardi N, *et al*. Axons and dendrites originate from neuroepithelial-like processes of retinal bipolar cells. Nat Neurosci, 2006, 9: 85–92
43 Naito J, Chen Y. Morphological features of chick retinal ganglion cells. Anat Sci Int, 2004, 79: 213–225
44 Naito J, Chen Y. Morphologic analysis and classification of ganglion cells of the chick retina by intracellular injection of Lucifer Yellow and retrograde labeling with DiI. J Comp Neurol, 2004, 469: 360–376
45 Urbanska M, Blazejczyk M, Jaworski J. Molecular basis of dendritic arborization. Acta Neurobiol Exp (Wars), 2008, 68: 264–288
46 Chan Y C, Chiao C C. Effect of visual experience on the maturation of ON-OFF direction selective ganglion cells in the rabbit retina. Vision Res, 2008, 48: 2466–2475
47 Lau K C, So K F, Tay D. Effects of visual or light deprivation on the morphology, and the elimination of the transient features during development, of type I retinal ganglion cells in hamsters. J Comp Neurol, 1990, 300: 583–592
48 Niell C M, Smith S J. Functional imaging reveals rapid development of visual response properties in the zebrafish tectum. Neuron, 2005, 45: 941–951
49 Tian N. Visual experience and maturation of retinal synaptic pathways. Vision Res, 2004, 44: 3307–3316
50 Tian N, Copenhagen D R. Visual stimulation is required for refinement of ON and OFF pathways in postnatal retina. Neuron, 2003, 39: 85–96